Paeonol alleviates lipopolysaccharide-induced hepatocytes injury through alteration of mitochondrial function and NF-κB translocation

SHOUZHU XU[1,2*], JIE XU[2*], TING HAO[2], YU YAN[2], SHIHAO ZHANG[2], AIHONG LI[1], CHUANDAO SHI[2], QILING LIU[2] and JING ZHAO[3,4]

[1]Shaanxi Pharmaceutical Holding Grp Co. Ltd., Shaanxi Pharmaceutical Dev Ctr, Xian, Shaanxi 710075, [2]Department of Public Health; [3]College of Acupuncture and Moxibustion and [4]Shaanxi Key Laboratory of Acupuncture and Medicine, Shaanxi University of Chinese Medicine, Xianyang, Shaanxi 712046, P.R. China

Received April 1, 2021; Accepted July 26, 2021

DOI: 10.3892/mmr.2021.12419

Abstract. Sepsis is a severe disease, with high mortality. Permanent organ damage caused by sepsis reduces the quality of life of surviving patients. The liver is an easily damaged organ in sepsis and sepsis-associated liver injury foretells a poor prognosis. Unfortunately, there are no effective treatments or drugs to solve this problem. Therefore, strategies or novel drugs are urgently required to protect against liver dysfunction in sepsis. In the present study, lipopolysaccharide (LPS) was used to establish a model of liver injury *in vitro*. The data demonstrated that pretreatment of L02 human normal hepatocytes with paeonol (PAE) alleviated LPS-induced cell injury and decreased the levels of alanine aminotransferase and aspartate transaminase, indicating a protective effect of PAE. Further experiments demonstrated that PAE increased LPS-decreased L02 cell viability, the levels of superoxide dismutase and Bcl-2 expression. PAE decreased LPS-increased cell apoptosis, intracellular reactive oxygen species and the expression levels of Bax and cleaved-caspase-3. PAE decreased LPS-promoted mitochondrial depolarization and nuclear translocation of NF-κB. In conclusion, PAE alleviated LPS-induced liver injury via alteration of mitochondrial function and NF-κB translocation. Therefore, PAE has potential for the treatment of sepsis.

Correspondence to: Mrs. Jing Zhao, College of Acupuncture and Moxibustion, Shaanxi University of Chinese Medicine, Shiji Ave, Xi'an-Xianyang New Economic Zone, Xianyang, Shaanxi 712046, P.R. China
E-mail: zhaojing_1207@126.com

Professor Aihong Li, Shaanxi Pharmaceutical Holding Grp Co. Ltd., Shaanxi Pharmaceutical Dev Ctr, 69 Keji 2nd Road, Xian, Shaanxi 710075, P.R. China
E-mail: 408503572@qq.com

*Contributed equally

Key words: paeonol, sepsis, liver injury, reactive oxygen species, nuclear translocation of NF-κB

Introduction

Sepsis is characterized by potentially fatal organ dysfunction, resulting from the abnormal immune response to an infection (1). In total, ~3 per 1,000 individuals are estimated to be diagnosed with severe sepsis (2). In sepsis, the abnormal expression of proinflammatory cytokines and chemokines is the driving force behind the development of septic shock, which results in an overt systemic inflammatory response and tissue injury (3). In addition to causing high mortality, sepsis causes a reduction in the quality of life for surviving patients, due to the permanent organ damage (4). The liver serves a fundamental role in hypermetabolism, generates acute phase proteins during the inflammatory response and is of great importance in bacteria clearance and host defense (5,6). Furthermore, the liver is an easily damaged organ in sepsis and sepsis-associated liver injury forecasts a poor prognosis in patients with sepsis (7). Therefore, protection against liver injury during sepsis is of great importance.

Paeonol (PAE; 2'-hydroxy-4'-methoxyacetophenone) is one of the major components extracted from *Dioscorea japonica*, *Paeonia suffruticosa*, *Paeonia lactiflora* and *Arisaema erubescens* (8-10). PAE has numerous biological functions, such as antioxidant, anti-inflammatory and cardiovascular protection (11). In addition to the aforementioned properties, PAE reduces the mortality by confining high mobility group box 1 to the nucleus in lipopolysaccharide (LPS)-stimulated rats (12). However, the roles of PAE in liver protection remain to be elucidated. It was hypothesized that PAE could exert an important protective role in LPS-damaged hepatocytes. In the present study, LPS was used to induce injury in L02 human normal hepatocytes and the protective effect of PAE was observed using different methods as subsequently described.

Materials and methods

Cell culture and drug treatment. L02 human normal hepatocytes were purchased from BioVector NTCC Inc. and the cells were cultured in a 5% CO_2 atmosphere at 37˚C. The cells were maintained in DMEM (Gibco; Thermo Fisher Scientific, Inc.) supplemented with 10% (v/v) FBS (Cellmax; Lanzhou Minhai Bio-engineering Co., Ltd.), 100 U/ml streptomycin and 100 U/ml penicillin. The cells were seeded into 6-, 24- or 96-well culture dishes and serum-starved for 12 h in DMEM when the cells had reached sub-confluence. Cells treated with DMEM were used as a control group. Hepatocyte injury was induced by incubation with LPS (cat. no. ST1470-10 mg; Beyotime Institute of Biotechnology). PAE (cat. no. B20266; Shanghai Yuanye Bio. Tech. Co., Ltd.) was added to the cells 1 h prior to LPS stimulation. In the present study, a ScienCell HeLa Cell Contamination Detection kit (cat. no. 8988; ScienCell Research Laboratories, Inc.) was used for the detection of HeLa cell contamination in cultured L02 cells by PCR. The data demonstrated that L02 cells had no detectable HeLa cell contamination (Fig. 1).

Cell viability assay. Cell viability was tested using a Cell Counting Kit-8 (CCK-8; cat. no. C0037; Beyotime Institute of Biotechnology) according to the manufacturer's instructions. A total of $1.5x10^3$ cells/well were seeded into a 96-well plate and then serum-starved for 12 h in DMEM when the cells had reached sub-confluence. The cells were incubated with different concentrations of LPS (0.05, 0.5, 5.0 or 10.0 μg/ml), incubated with different concentrations of PAE (0.1, 1.0, 10.0 or 100.0 μg/ml) for 12 h or incubated with different concentrations of PAE (0.1, 1.0 or 10.0 μg/ml) for 1 h and then co-cultured with LPS (10 μg/ml) for 12 h in a 5% CO_2 atmosphere. All incubations were at 37˚C. Following the indicated treatment, 10 μl CCK-8 solution was added to each well. The cells were then incubated at 37˚C for 4 h and the absorbance value was determined at 450 nm using a microplate reader (Bio-Rad Laboratories, Inc.). Each experiment was repeated six times.

Measurements of alanine aminotransferase (ALT) and aspartate transaminase (AST) activity. Hepatocyte damage was examined by measuring the activities of ALT (U/g protein; cat. no. C010-2-1; Nanjing Jiancheng Bioengineering Institute) and AST (U/g protein; cat. no. C009; Nanjing Jiancheng Bioengineering Institute) using ALT and AST assay kits. Briefly, $1x10^6$ cells were seeded into 24-well plates and serum-starved for 12 h in DMEM when the cells had reached sub-confluence. Subsequently, cells were incubated with LPS (10.0 μg/ml) or incubated with PAE (10.0 μg/ml) for 1 h and then co-incubated with LPS (10 μg/ml) for 12 h, separately. The activities of ALT and AST were assayed according to the manufacturer's instructions.

Cellular apoptosis assay. The apoptosis assay was carried out using an Annexin V-FITC apoptosis detection kit (cat. no. C1067s; Beyotime Institute of Biotechnology). Briefly, $1x10^6$ cells were seeded in Nunc glass bottom dishes and then serum-starved for 12 h in DMEM when the cells had reached sub-confluence. Subsequently, cells were incubated with LPS (10.0 μg/ml) or incubated with PAE (10.0 μg/ml) for 1 h and then co-incubated with LPS (10 μg/ml) for 12 h at 37˚C in a 5% CO_2 atmosphere, separately. Following treatment, cells were washed with PBS three times and 5 μl FITC-labeled Annexin V and 195 μl binding buffer were added into each dish. The dishes were then incubated in the dark for 10 min at 25˚C. This was followed by incubation with 10 μl propidium iodide in the dark for another 20 min at 4˚C. Apoptotic cells were observed using laser confocal microscopy (original magnification, x200). The cell population was separated into three groups: Live cells with low fluorescence, early apoptotic cells stained with green fluorescence and necrotic/advanced stage apoptotic cells stained with both red and green fluorescence.

Western blotting. Cells ($5\text{-}7x10^6$/well) were seeded into 6-well plates and serum-starved for 12 h in DMEM when the cells had reached sub-confluence. Subsequently, cells were incubated with LPS (10.0 μg/ml) or incubated with PAE (10.0 μg/ml) for 1 h and then co-incubated with LPS (10 μg/ml) for 12 h, separately. Following treatment, cells were washed with ice-cold PBS three times and solubilized with 200 μl ice-cold lyse buffer (cat. no. P0013C; Beyotime Institute of Biotechnology). Subsequently, supernatants were collected by centrifugation at 12,000 x g for 10 min at 4˚C, and the concentration of protein was identified by the BCA method (cat. no. AR1189; Boster Biological Technology). Loading buffer was added into each supernatant followed by boiling for 8 min. Lysate (30 μg) was electrophoresed on a 12% SDS-PAGE gel and transferred onto a nitrocellulose membrane. The membrane was blocked with 5% bovine serum albumin (Sigma-Aldrich; Merck KGaA) overnight at 4˚C. The blots were incubated with antibodies against Bcl-2 (dilution, 1:8,000; cat. no. AB112; Beyotime Institute of Biotechnology), Bax (dilution, 1:5,000; cat. no. AF0054; Beyotime Institute of Biotechnology), cleaved-caspase-3 (dilution, 1:5,000; cat. no. 9661s; Cell Signaling Technology, Inc.) or β-actin (dilution, 1:10,000; cat. no. NC011; Zhuangzhi Biotech.) overnight at 4˚C and then the membranes were incubated at 25˚C for 3 h with goat anti-mouse IgG-HRP (1:5,000; cat. no. sc-2005) or goat anti-rabbit IgG-HRP (1:5,000; cat. no. sc-2004); these secondary antibodies were purchased from Santa Cruz Biotechnology, Inc. The immune complexes were enhanced by chemiluminescence (cat. no. WBULS0500; Merck Life Science UK, Ltd.). The results were analyzed using Quantity One software (Bio-Rad Laboratories, Inc.; version 6.0Inc.).

Measurement of mitochondrial transmembrane potential. A JC-1 probe (cat. no. C2006; Beyotime Institute of Biotechnology) was used to measure mitochondrial depolarization according to the manufacturer's protocol. Briefly, $1x10^6$ cells were seeded into Nunc glass bottom dishes and serum-starved for 12 h in DMEM when the cells had reached sub-confluence. Subsequently, cells were incubated with LPS (10.0 μg/ml) or incubated with PAE (10.0 μg/ml) for 1 h and then co-incubated with LPS (10 μg/ml) for 12 h at 37˚C in a 5% CO_2 atmosphere, separately. Following treatment, cells were incubated at 37˚C for 20 min with 25 μg/ml JC-1, then washed twice with PBS and placed

in fresh DMEM without serum. Mitochondrial membrane potentials were monitored by observing the relative amounts of dual emissions from mitochondrial JC-1 monomers or aggregates using laser confocal microscopy. Mitochondrial depolarization was indicated by an increase in the green fluorescence intensity.

Detection of intracellular reactive oxygen species (ROS). ROS were assayed with the probe 2',7'-dichlorofluorescein diacetate (DCFH-DA). DCFH-DA can easily diffuse into the cells and is deacetylated to nonfluorescent 2',7'-dichlorofluorescein (DCFH) by esterases. DCFH reacts with intracellular ROS to form the fluorescent product DCF. Briefly, $1x10^6$ cells were seeded into Nunc glass bottom dishes and serum-starved for 12 h in DMEM when the cells had reached sub-confluence. Subsequently, cells were incubated with LPS (10.0 μg/ml) or incubated with PAE (10.0 μg/ml) for 1 h and then co-incubated with LPS (10 μg/ml) for 4 h at 37˚C in a 5% CO_2 atmosphere, separately. Following treatment, the culture medium was removed and the cells were washed three times with PBS. DCFH-DA (10 μM) was added into the dishes and the cells were then incubated for an additional 20 min at 37˚C. The fluorescence was observed with a laser confocal microscope (original magnification, x200).

Determination of Cu/Zn superoxide dismutase (SOD) and Mn SOD activities. The enzyme activities of SOD were determined using a Cu/Zn SOD and Mn-SOD assay kit (cat. no. S0103; Beyotime Institute of Biotechnology) according to the manufacturer's instructions. In brief, $1x10^6$ cells/well were seeded in 24-well plates and serum-starved for 12 h in DMEM when the cells had reached sub-confluence. Then, cells were incubated with LPS (10.0 μg/ml) or incubated with PAE (10.0 μg/ml) for 1 h and then co-incubated with LPS (10 μg/ml) for 12 h at 37˚C in a 5% CO_2 atmosphere, separately. Following treatment, Cu/Zn-SOD inhibitors were added into cell lysates, followed by incubation for 30 min at 37˚C and mixing with WST-8 enzyme for another 30 min at 37˚C. The absorbance at 450 nm was assessed using a multimode microplate reader (Thermo Fisher Scientific, Inc.). The results were calculated and normalized to the protein concentration of each sample (U/g protein).

Lipid peroxidation assay. Lipid peroxidation was measured by detecting the content of thiobarbituric acid reactive substances using a lipid peroxidation malondialdehyde (MDA) assay kit (cat. no. S0131S; Beyotime Institute of Biotechnology). In brief, $1x10^6$ cells were seeded into 24-well plates and serum-starved for 12 h in DMEM when the cells had reached sub-confluence. The cells were then incubated with LPS (10.0 μg/ml) or incubated with PAE (10.0 μg/ml) for 1 h and then co-incubated with LPS (10 μg/ml) for 12 h at 37˚C in a 5% CO_2 atmosphere, separately. After the indicated treatment, 0.2 ml MDA detection agent was added into 0.1 ml cell lysate and then the mixture was heated in a water bath at 100˚C for 15 min. After cooling to room temperature, the mixture was centrifuged at 150 x g for 10 min. The supernatant (200 μl) was added to a 96-well plate and the absorbance at 532 nm was measured using a microplate reader (Thermo Fisher Scientific, Inc.). The levels of MDA were calculated from the standard graph of known concentrations of MDA and presented as μmol/g protein.

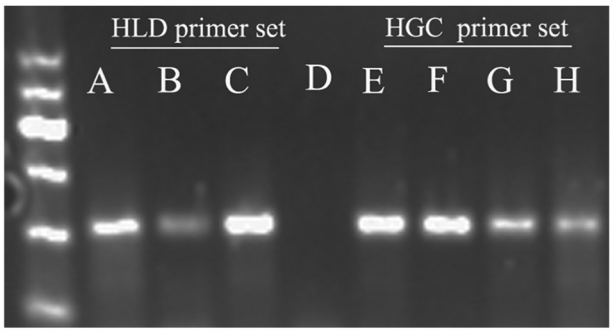

Figure 1. Gel electrophoresis separation of PCR products. (A-D) PCR products of genomic DNA samples by using HeLa gDNA detection primer set. (E-H) products of genomic DNA samples by using Human gDNA control primer set. (A and E) HeLa positive control PCR template, (B and F) HeLa cells, (C and G) L02 cells mixed with 1% HeLa cells and (D and H) L02 cells. HLD, HeLa gDNA detection primer set; HGC, Human gDNA control primer set.

Assay of the nuclear translocation of NF-κB using immunofluorescence staining. The NF-κB activation nuclear translocation assay kit (cat. no. SN368; Beyotime Institute of Biotechnology) was used to measure NF-κB activation. In brief, $1x10^6$ cells were seeded into Nunc glass bottom dishes and serum-starved for 12 h in DMEM when the cells had reached sub-confluence. Then, cells were incubated with LPS (10.0 μg/ml) or incubated with PAE (10.0 μg/ml) for 1 h and then co-incubated with LPS (10 μg/ml) for 12 h at 37˚C in a 5% CO_2 atmosphere, separately. Following treatment, cells on plates were washed with PBS once, fixed with 4% paraformaldehyde for 20 min at 25˚C, washed three times with PBS and blocked with 5% bovine serum albumin for 1.5 h at room temperature. Afterwards, they were incubated with the primary rabbit anti-NF-κB p65 antibody at 4˚C for 24 h, followed by incubation with Cy3-labeled secondary antibody at 25˚C for 2 h. Subsequently, the cells were stained with DAPI solution for 8 min. Each aforementioned step was followed by washing three times for 5 min. The activation or nuclear translocation of NF-κB was observed by laser confocal microscopy (original magnification, x200).

Statistical analysis. The data are presented as the mean ± SEM. The normality and homogeneity of these data were tested by Shapiro-Wilk tested, $P>0.05$ was considered to normal distribution. The differences among groups were assessed by a one-way ANOVA followed by a Dunnett's post hoc test or non-parametric Kruskal-Wallis followed by Dunn's test analysis using GraphPad Prism 8.3 software (GraphPad Software, Inc.). $P<0.05$ was considered to indicate a statistically significant difference.

Results

PAE increases LPS-decreased cell viability. In the present study, a cell viability assay was performed to select the appropriate concentrations of PAE and LPS. LPS at 0.5 μg/ml markedly decreased the cell viability in a concentration-dependent manner (Fig. 2A). However, treatment of

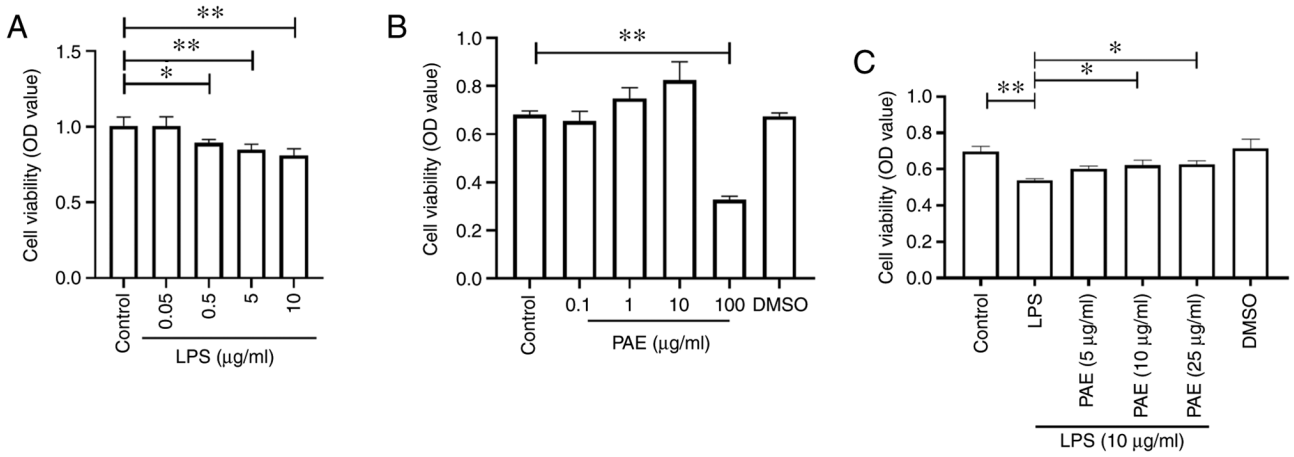

Figure 2. PAE increases LPS decreased cell viability of L02 cells. (A) The injury effect of LPS on cell viability of L02 cells. Cells were incubated with different concentration of LPS (0.05, 0.5, 5.0 or 10.0 μg/ml) for 12 h. (B) The effect of PAE alone on cell viability of L02 cells. Cells were incubated with different concentration of PAE (0.1, 1.0, 10.0 or 100.0 μg/ml) for 12 h. (C) The protective effect of PAE on LPS damaged L02 cells. Cells were incubated with different concentration of PAE (0.1, 1.0 or 10.0 μg/ml) prior 1 h and then co-incubated with LPS (10 μg/ml) for 12 h. Cell viability was assessed by CCK-8. Data represent mean ± standard error of the mean of six independent experiments. *P<0.05 or **P<0.01 vs. control or LPS. PAE, paeonol; LPS, lipopolysaccharide.

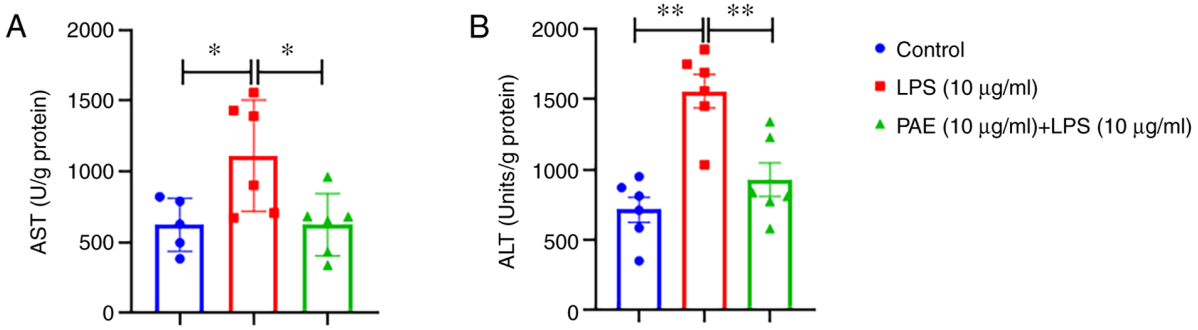

Figure 3. PAE inhibits LPS increased ALT and AST of L02 cells. Cells were incubated with LPS at 10.0 μg/ml for 12 h or cells were incubated with PAE at 10.0 μg/ml prior 1 h and then co-incubated with LPS (10 μg/ml) for 12 h. The activities of (A) ALT and (B) AST were assayed according to the manufacturer's instructions. Data represent mean ± standard error of the mean of six independent experiments. *P<0.05 or **P<0.01 vs. control. PAE, paeonol; LPS, lipopolysaccharide; ALT, alanine aminotransferase; AST, aspartate transaminase.

the cells with PAE at 0.1-10 μg/ml for 12 h had no effect on cell viability (Fig. 2B). Fig. 2C indicated that incubation with PAE at 1.0-10.0 μg/ml for 1 h followed by co-incubation with LPS (10 μg/ml) for 12 h could increase LPS-decreased cell viability. Therefore, 10.0 μg/ml PAE and 10 mg/ml LPS were used for subsequent experiments.

PAE decreases LPS-increased ALT and AST levels. Hepatocellular damage results in the release of the intracellular enzymes ALT and AST. The results in Fig. 3 indicated that PAE pretreatment reduced LPS-induced levels of liver enzymes (ALT and AST).

PAE inhibits LPS-induced cell apoptosis. To further evaluate the protective effect of PAE on LPS-induced L02 cell injury, an Annexin V/PI double staining assay was performed. The results in Fig. 4 revealed that only a few cells could be stained green (early apoptotic cells) or red (late apoptotic cells) in the control group, while an increasing number of early apoptotic (stained in green) and/or necrotic (late apoptotic; stained in red) cells were observed following treatment with LPS for 12 h. Furthermore, pretreatment of the cells with PAE for 1 h prior to LPS stimulation could markedly decrease cell apoptosis, which suggested that PAE exerted a protective effect on LPS-induced cell injury.

PAE decreases LPS-increased expression levels of Bax and cleaved-caspase-3 and increases the expression levels of Bcl-2. The results in Fig. 5 indicated that Bax and cleaved-caspase-3 expression was increased following the treatment of cells with LPS for 12 h (P<0.05 vs. control). Pretreatment of the cells with PAE (10 μg/ml) for 1 h prior to LPS stimulation markedly inhibited LPS-induced protein expression levels of Bax and cleaved-caspase-3. However, the expression levels of Bcl-2 were increased following the treatment with PAE. These results further indicated that PAE exerted a protective effect on LPS-induced cell apoptosis.

PAE decreases LPS-increased ROS formation. Based on the aforementioned results that PAE could restore LPS-injured cell apoptosis, the present study further detected intracellular ROS levels to assess the anti-oxidative activity of PAE. Cells treated with LPS for 4 h exhibited an increase in the

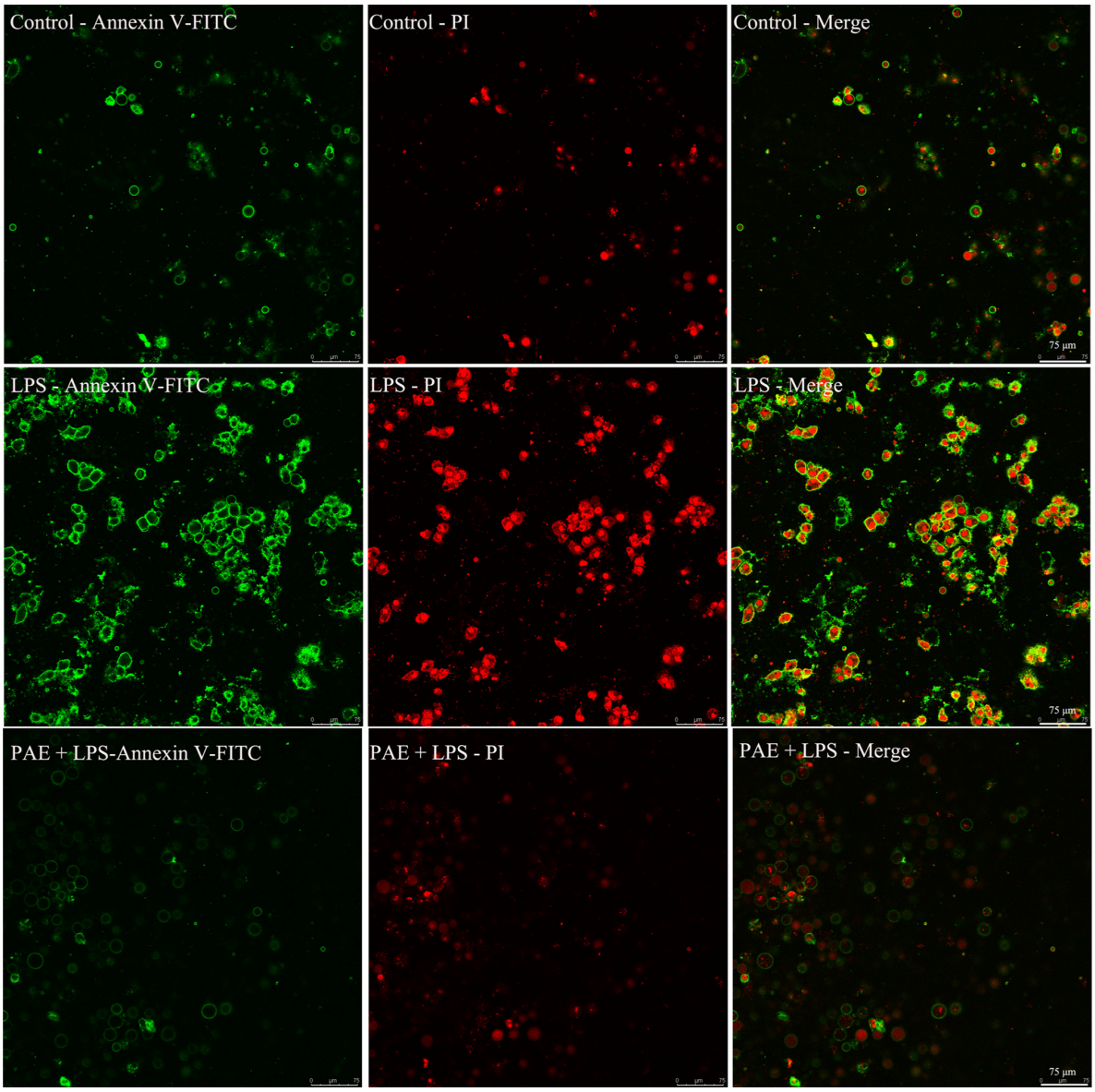

Figure 4. PAE inhibits LPS induced the apoptosis of L02 cells. Cells were incubated with LPS at 10.0 μg/ml for 12 h or cells were incubated with PAE at 10.0 μg/ml prior 1 h and then co-incubated with LPS (10 μg/ml) for 12 h. Cell apoptosis was observed with laser confocal microscopy (scale bar=75 μm). The population was separated into three groups: Live cells with a low level of fluorescence, apoptotic cells in the earlier period with green fluorescence and necrotic and advanced stage apoptotic cells with both red and green fluorescence. PAE, paeonol; LPS, lipopolysaccharide.

intensity of fluorescence. However, pretreatment with PAE (10 μg/ml) markedly decreased the intensity of fluorescence (Fig. 6), which demonstrated the anti-oxidative effects of PAE.

PAE decreases LPS-increased MDA levels and increases LPS-decreased SOD levels. Given the important role of oxygen free radicals in the pathogenesis of liver injury, MDA and SOD levels were examined. As shown in Fig. 7, LPS markedly increased MDA levels and decreased SOD levels. Furthermore, pretreatment of the cells with PAE could markedly decrease the levels of MDA and tended to increase the SOD levels (P=0.182).

PAE increases the LPS-decreased mitochondrial transmembrane potential. The protective effect of PAE on LPS-induced L02 cell injury was further assayed by detecting mitochondrial depolarization. The control cells stained with JC-1 emitted mitochondrial red fluorescence with weak green fluorescence (Fig. 8), indicating hyperpolarized mitochondria. However, cells treated with LPS exhibited increased green fluorescence and weakened red fluorescence, indicating the depolarization of mitochondria. Compared with that in the LPS-damaged group, PAE relieved the LPS-induced mitochondrial depolarization, as indicated by the fluorescent color changes from green to red.

PAE inhibits LPS-induced nuclear translocation of NF-κB. To further investigate the protective effect of PAE on LPS-induced cell injury, the NF-κB levels in the nuclei of L02 cells were detected using immunofluorescence staining. The immunofluorescence staining revealed that LPS promoted NF-κB translocation into the nuclei of L02 cells. As shown in Fig. 9, the p65 subunit was translocated to the nucleus (the

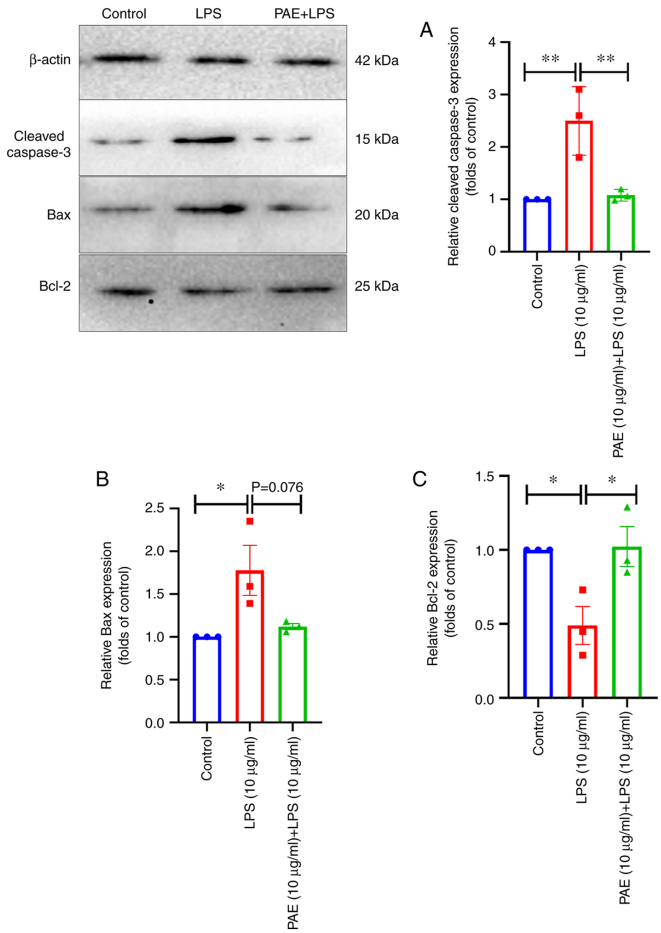

Figure 5. PAE decreases LPS-increased the expression of Bax and caspase-3, increases the level of Bcl-2. Cells were incubated with LPS at 10.0 μg/ml for 12 h or cells were incubated with PAE at 10.0 μg/ml prior 1 h and then co-incubated with LPS (10 μg/ml) for 12 h. (A) Cleaved-casapse-3, (B) Bax and (C) Bcl-2 were assayed by western blotting. Data represent mean ± standard error of the mean of six independent experiments. *P<0.05 or **P<0.01 vs. control. PAE, paeonol; LPS, lipopolysaccharide.

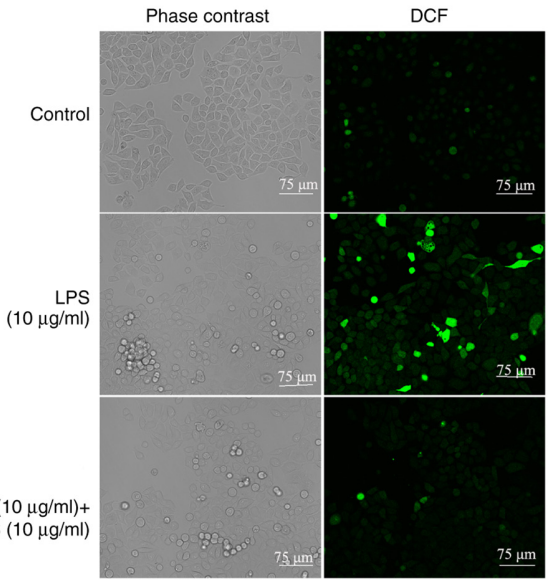

Figure 6. PAE decreases LPS induced ROS generation of L02 cells (bar=75μm). Cells were incubated with LPS at 10.0 μg/ml for 12 h or cells were incubated with PAE at 10.0 μg/ml prior 1 h and then co-incubated with LPS (10 mg/ml) for 4 h. Intracellular ROS was observed with laser confocal microscopy. The population was separated into two groups: Left panels were cells observed by phase contrast and right panels were cells observed by fluorescence microscopy. PAE, paeonol; LPS, lipopolysaccharide; ROS, reactive oxygen species; DCF, dichlorofluorescein.

red fluorescence in the nucleus was intense in most cells). Following the treatment with PAE, the intensity of the red fluorescence was faint, especially in the nucleus. These results further suggested that PAE exerted protective effects on LPS-induced cell injury by inhibiting NF-κB transduction.

Discussion

The systemic inflammatory response and multi-organ dysfunction are the main features of sepsis (13). The liver is the second organ easily injured during sepsis and liver injury indicates poor prognosis in patients with sepsis (14). Liver dysfunction is closely associated with the mortality rate of sepsis and early liver dysfunction is an independent risk factor for poor prognosis (15). Therefore, protection against liver injury is important for the treatment of sepsis. LPS is the main surface molecule of most gram-negative bacteria and routinely used to establish sepsis models both *in vivo* and *in vitro* (16). The present study demonstrated that LPS markedly decreased cell viability of hepatocytes, increased ALT, AST, intracellular ROS levels and cell apoptosis and promoted mitochondrial depolarization and NF-κB translocation into the nucleus, all of which suggested an established *in vitro* liver injury model of sepsis.

ALT and AST levels tend to increase when liver damage occurs (17). The present results indicated that PAE pretreatment considerably reduced the levels of liver enzymes (ALT and AST). MDA is the final product of lipid peroxidation and SOD is one of the most important antioxidant enzymes, with high endogenous expression in the liver, that eliminates toxic free radicals (18,19). The present data demonstrated that PAE pretreatment markedly reduced the levels of MDA and increased SOD activity, suggesting an antioxidant effect of PAE. ROS serve a crucial role in cell injury induction under both physiological and pathological conditions (20). ROS are mainly generated in the mitochondria and unbalanced ROS generation results in the loss of mitochondrial membrane potential (21). The mitochondrial depolarization leads to the release of intermembrane proteins, such as cytochrome c, which ultimately induces caspase-3 activation (22). The activation of caspase-3 leads to DNA breakage, nuclear chromatin condensation and cell apoptosis (23). Anti-apoptotic Bcl-2 and proapoptotic Bax are upstream of mitochondria and Bcl-2 can inhibit the mitochondrial depolarization and ROS production, while Bax exerts the opposite function (24). Consistent with these results, the present data demonstrated that LPS increased intracellular ROS, induced mitochondrial depolarization, increased the expression levels of cleaved-caspase-3 and Bax and decreased the expression levels of Bcl-2. However, prior incubation of the cells with PAE attenuated LPS-induced high expression of Bax and cleaved-caspase-3, mitochondrial depolarization and increased Bcl-2 expression.

NF-κB is an activator in cell injury. Under normal conditions, NF-κB exists in an inactive state in the cytosol

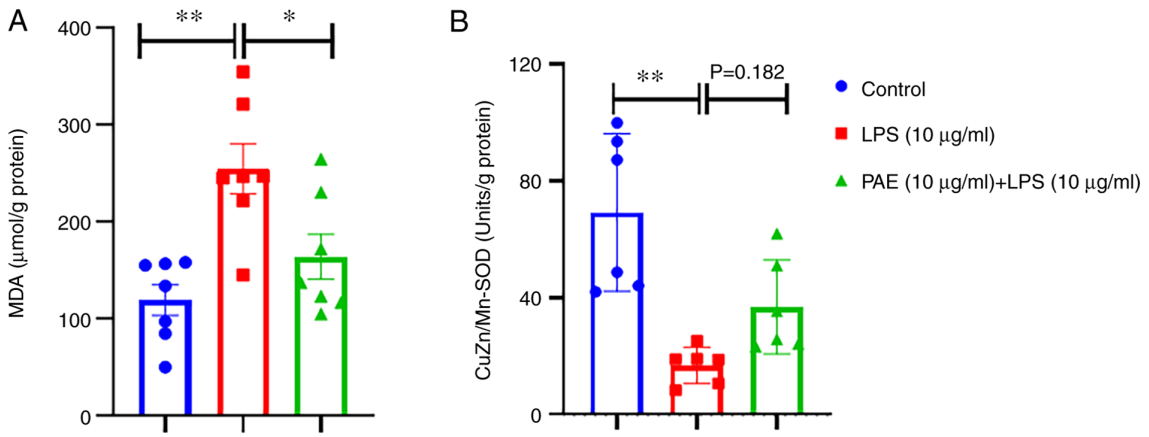

Figure 7. PAE inhibits LPS increased MDA and increases LPS decreased SOD level of L02 cells. Cells were incubated with LPS at 10.0 μg/ml for 12 h or cells were incubated with PAE at 10.0 μg/ml prior 1 h and then co-incubated with LPS (10 μg/ml) for 12 h. (A) MDA and (B) SOD were assayed by respective kits. Data represent mean ± standard error of the mean of six independent experiments. *P<0.05 or **P<0.01 vs. control. PAE, paeonol; LPS, lipopolysaccharide; MDA, malondialdehyde; SOD, superoxide dismutase.

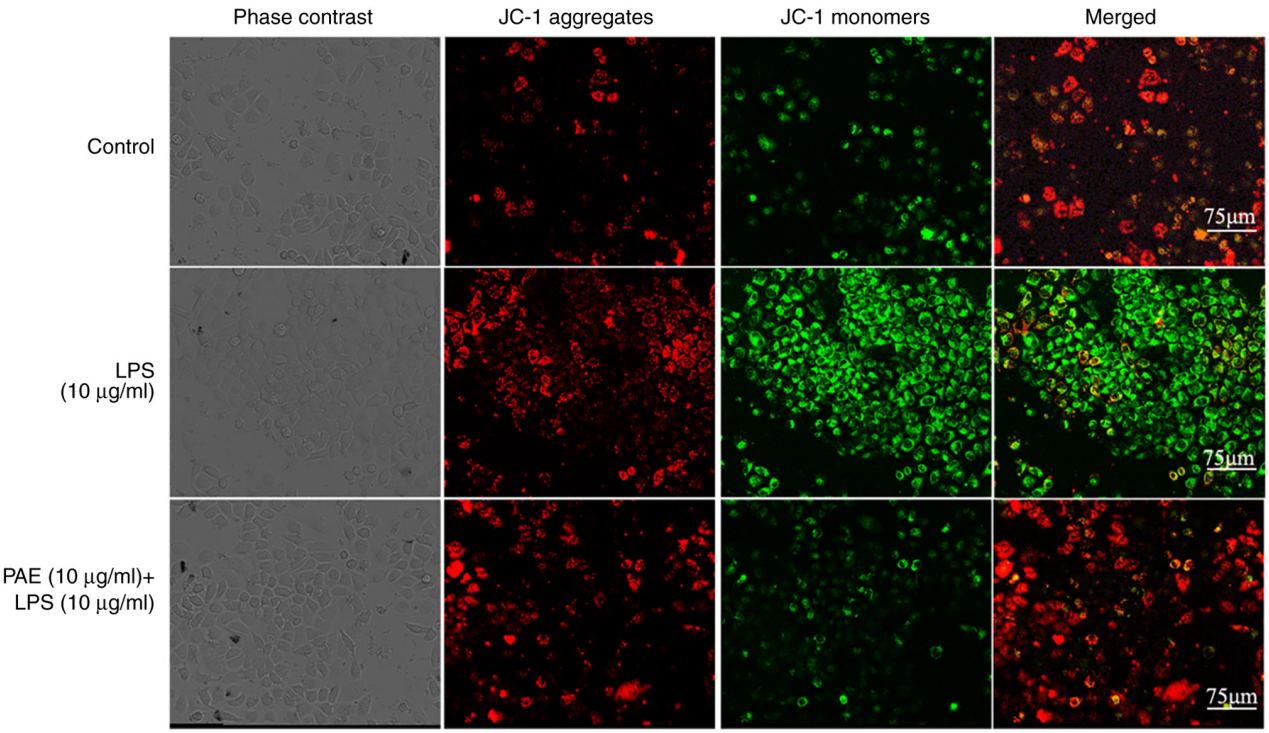

Figure 8. PAE increases LPS-decreased mitochondrial transmembrane potential in L02 cells (bar=75 μm). Cells were incubated with LPS at 10.0 μg/ml for 12 h or cells were incubated with PAE at 10.0 μg/ml prior 1 h and then co-incubated with LPS (μg/ml) for 12 h. The mitochondrial membrane potential was measured by laser confocal microscopy. The population was separated into four groups: Left panels were cells observed by bright light and right panels were the merged field of red (for JC-1 aggregates) and green color (for JC-1 monomers). PAE, paeonol; LPS, lipopolysaccharide.

by binding to NF-κB (25). Research has demonstrated that upon stimulation by LPS, NF-κB p65 is phosphorylated on serine-536 and the phosphorylated NF-κB enters the nucleus and regulates the secretion of pro-inflammatory cytokines to further amplify NF-κB activation (26,27). In the present study, LPS markedly increased NF-κB phosphorylation in L02 cells and PAE inhibited NF-κB nuclear translocation. The present results suggested that PAE ameliorated the injury of hepatocytes by mediating NF-κB activation.

In conclusion, PAE could mitigate LPS-induced hepatocyte injury, as demonstrated by decreased AST and ALT levels, as well as improved mitochondrial dysfunction, along with decreased superoxide production in mitochondria and NF-κB nuclear translocation and also decreased protein expression of apoptosis-related proteins. It should be noted that the current study has examined only on an *in vitro* model of LPS-induced hepatocyte and further research still needed especially explore the receptors, other signaling and the protective effect in an *in vivo* model. Notwithstanding its limitation, this study does confirm that PAE alleviated LPS-induced hepatocyte injury through the alteration of mitochondrial function and NF-κB translocation (see graphical abstract, Fig. 10).

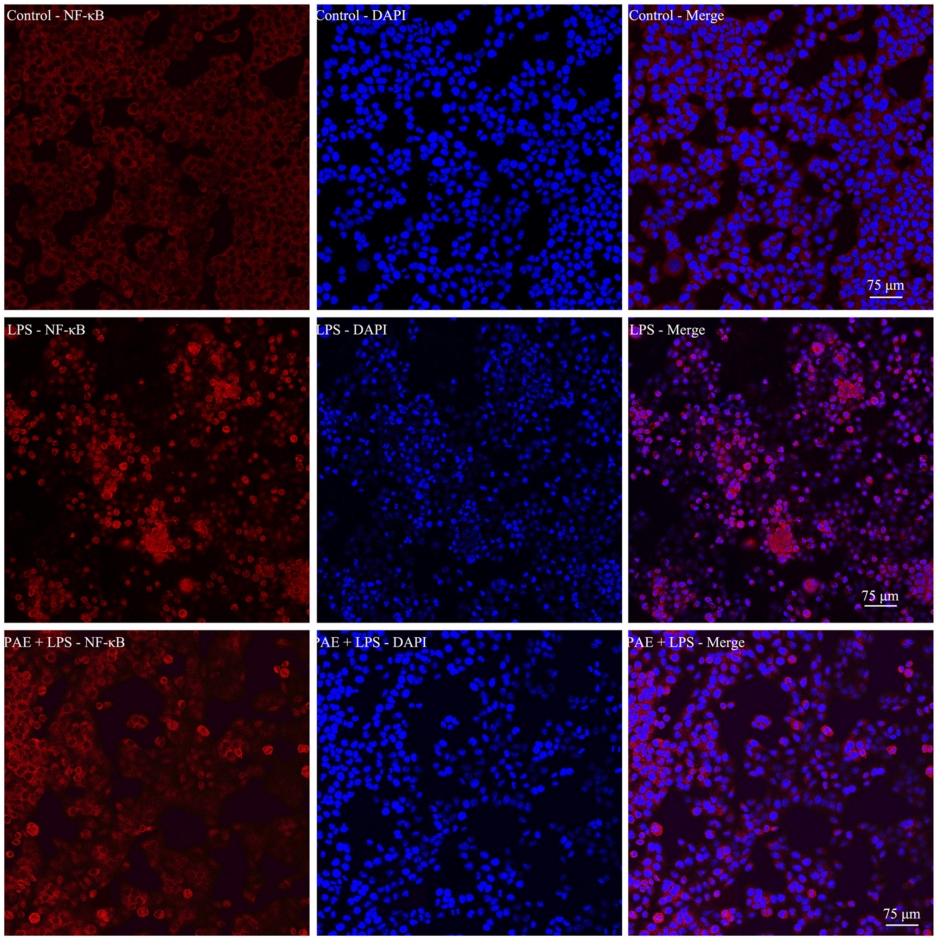

Figure 9. PAE inhibits LPS-promoted nuclear translocation of NF-κB (scale bar=75 μm). Cells were incubated with LPS at 10.0 μg/ml for 12 h or cells were incubated with PAE at 10.0 μg/ml prior 1 h and then co-incubated with LPS (10 μg/ml) for 12 h. The NF-κB level in the nuclei of L02 cells was detected by immunofluorescence staining. The right panels were the merged field of red (for NF-κB subunit p 65) and blue color (for cell nucleus). PAE, paeonol; LPS, lipopolysaccharide.

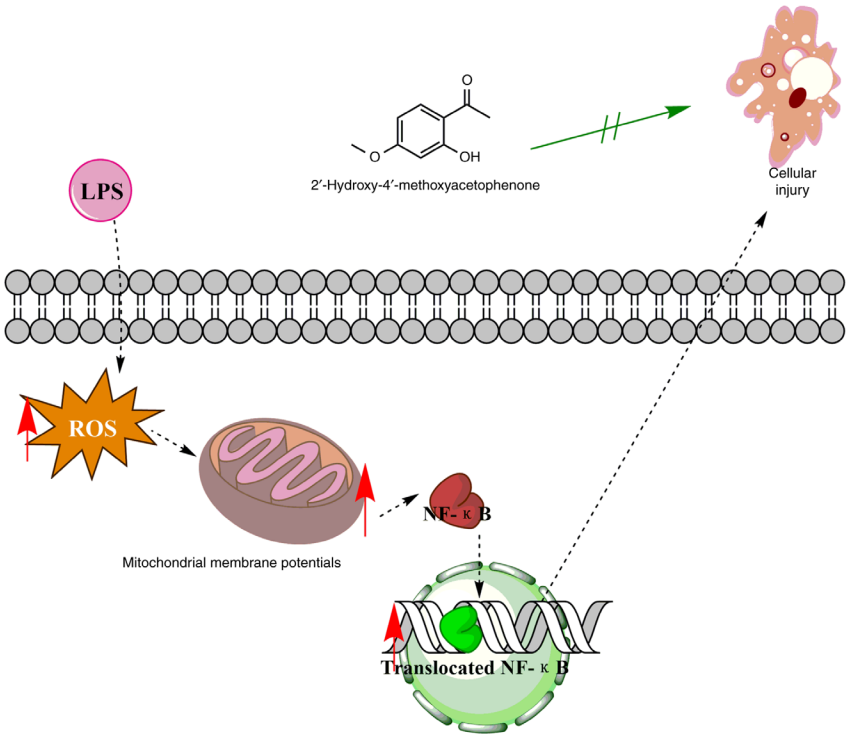

Figure 10. PAE alleviates LPS-induced hepatocytes injury through alteration of mitochondrial function and NF-κB translocation. PAE, paeonol; LPS, lipopolysaccharide; ROS, reactive oxygen species.

Acknowledgements

Not applicable.

Funding

The present study was sponsored by Key Research and Development Program of Shaanxi (program no. 2021SF-071). The National Training Program of Innovation and Entrepreneurship for Students of China (grant nos. 201910716019 and 201910716020), the Research Project of the Shaanxi University of Chinese Medicine (grant no. 2020GP19), the Scientific Research Fund Project of Shaanxi Province Department of Education (grant no. 19JK0228), Subject Innovation Team of Shaanxi University of Chinese Medicine (grant no. 2019-QN07/132041933) and Project of the Extension of Science and Technology of Xianyang City (grant no. 2019KT-11).

Availability of data and materials

The datasets used and/or analyzed during the current study are available from the corresponding author on reasonable request.

Authors' contributions

SX and JZ made substantial contributions to the conception and design of the study. YY, JX, TH and SZ acquired, analyzed and interpreted the data. JZ and AL confirmed the authenticity of all the raw data, and with CS and QL, further interpreted the data, drafted the article and revised it critically for important intellectual content. All authors read and approved the final manuscript.

Ethics approval and consent to participate

Not applicable.

Patient consent for publication

Not applicable.

Competing interests

The authors declare that they have no competing interests. In the present study, the cell culture of LO2 was performed in Shaanxi Pharmaceutical Holding Grp Co Ltd.

References

1. Theertha M, Sanju S, Priya VV, Jain P, Varma PK and Mony U: Innate lymphoid cells: Potent early mediators of the host immune response during sepsis. Cell Mol Immunol 17: 1114-1116, 2020.
2. Vakkalanka JP, Harland KK, Swanson MB and Mohr NM: Clinical and epidemiological variability in severe sepsis: An ecological study. J Epidemiol Community Health 72: 741-745, 2018.
3. Cohen J: Mechanisms of tissue injury in sepsis: Contrasts between gram positive and gram negative infection. J Chemother 13 Spec No 1: 153-158, 2001.
4. Sygitowicz G and Sitkiewicz D: Molecular mechanisms of organ damage in sepsis: An overview. Braz J Infect Dis 24: 552-560, 2020.
5. Yan J, Li S and Li S: The role of the liver in sepsis. Int Rev Immunol 33: 498-510, 2014.
6. Hensley MK and Deng JC: Acute on chronic liver failure and immune dysfunction: A mimic of sepsis. Semin Respir Crit Care Med 39: 588-597, 2018.
7. Woznica EA, Inglot M, Woznica RK and Lysenko L: Liver dysfunction in sepsis. Adv Clin Exp Med 27: 547-551, 2018.
8. Wu CF: A review on the pharmacology of Paeonia lactiflora and its chemical components. Zhong Yao Tong Bao 10: 43-45, 1985 (In Chinese).
9. Ducki S, Hadfield JA, Lawrence NJ, Zhang X and McGown AT: Isolation of paeonol from Arisaema erubescens. Planta Med 61: 586-587, 1995.
10. Adki KM and Kulkarni YA: Chemistry, pharmacokinetics, pharmacology and recent novel drug delivery systems of paeonol. Life Sci 250: 117544, 2020.
11. Zhang L, Li DC and Liu LF: Paeonol: Pharmacological effects and mechanisms of action. Int Immunopharmacol 72: 413-421, 2019.
12. Liu X, Xu Q, Mei L, Lei H, Wen Q, Miao J, Huang H, Chen D, Du S, Zhang S, *et al*: Paeonol attenuates acute lung injury by inhibiting HMGB1 in lipopolysaccharide-induced shock rats. Int Immunopharmacol 61: 169-177, 2018.
13. Opal SM: Severe sepsis and septic shock: Defining the clinical problem. Scand J Infect Dis 35: 529-534, 2003.
14. Oswari H, Widjaja RK, Rohsiswatmo R and Cleghorn G: Prognostic value of biochemical liver parameters in neonatal sepsis-associated cholestasis. J Paediatr Child Health 49: E6-E11, 2013.
15. Kim TS and Choi DH: Liver dysfunction in sepsis. Korean J Gastroenterol 75: 182-187, 2020.
16. Iketani M, Ohshiro J, Urushibara T, Takahashi M, Arai T, Kawaguchi H and Ohsawa I: Preadministration of hydrogen-rich water protects against Lipopolysaccharide-induced sepsis and attenuates liver injury. Shock 48: 85-93, 2017.
17. Webster GF, Webster TG and Grimes LR: Laboratory tests in patients treated with isotretinoin: Occurrence of liver and muscle abnormalities and failure of AST and ALT to predict liver abnormality. Dermatol Online J 23: 2017.
18. Long J, Wang X, Gao H, Liu Z, Liu C, Miao M and Liu J: Malonaldehyde acts as a mitochondrial toxin: Inhibitory effects on respiratory function and enzyme activities in isolated rat liver mitochondria. Life Sci 79: 1466-1472, 2006.
19. El-Shabrawi MH, Kamal NM, Halawa FA, El-Guindi MA and Sobhy GA: Serum superoxide dismutase activity in acute and chronic paediatric liver diseases. Arab J Gastroenterol 15: 72-75, 2014.
20. Silwal P, Kim JK, Kim YJ and Jo EK: Mitochondrial reactive oxygen species: Double-edged weapon in host defense and pathological inflammation during infection. Front Immunol 11: 1649, 2020.
21. Forrester SJ, Kikuchi DS, Hernandes MS, Xu Q and Griendling KK: Reactive oxygen species in metabolic and inflammatory signaling. Circ Res 122: 877-902, 2018.
22. Sanderson TH, Reynolds CA, Kumar R, Przyklenk K and Huttemann M: Molecular mechanisms of ischemia-reperfusion injury in brain: Pivotal role of the mitochondrial membrane potential in reactive oxygen species generation. Mol Neurobiol 47: 9-23, 2013.
23. Abu-Qare AW and Abou-Donia MB: Biomarkers of apoptosis: Release of cytochrome c, activation of caspase-3, induction of 8-hydroxy-2'-deoxyguanosine, increased 3-nitrotyrosine and alteration of p53 gene. J Toxicol Environ Health B Crit Rev 4: 313-332, 2001.
24. D'Orsi B, Mateyka J and Prehn JH: Control of mitochondrial physiology and cell death by the Bcl-2 family proteins Bax and Bok. Neurochem Int 109: 162-170, 2017.
25. Baker RG, Hayden MS and Ghosh S: NF-κB, inflammation and metabolic disease. Cell Metab 13: 11-22, 2011.
26. Zhang G and Ghosh S: Molecular mechanisms of NF-kappaB activation induced by bacterial lipopolysaccharide through Toll-like receptors. J Endotoxin Res 6: 453-457, 2000.
27. Hwang CJ, Park MH, Hwang JY, Kim JH, Yun NY, Oh SY, Song JK, Seo HO, Kim YB, Hwang DY, *et al*: CCR5 deficiency accelerates lipopolysaccharide-induced astrogliosis, amyloid-beta deposit and impaired memory function. Oncotarget 7: 11984-11999, 2016.